Joint Pathology Center
Veterinary Pathology Services

WEDNESDAY SLIDE CONFERENCE 2021-2022

C o n f e r e n c e 16

26 January 2022

CASE I:

Signalment:
4-month old, male common marmoset (*Callithrix jacchus*)

History:
This 4-month old, male marmoset presented for being down in his cage and unresponsive. On physical exam, he was noted to be laterally recumbent, hypothermic, and dehydrated. The animal was minimally responsive to repeated supportive care attempts, and humane euthanasia was elected, followed by a necropsy. Prior to presentation, a sibling in this same family was submitted for necropsy, where postmortem culture and subsequent serotyping identified *Salmonella typhimurium*.

Gross Pathology:
At necropsy, the stomach was filled with tan to white feed material. The small intestines were variably distended with gas and contained scant to moderate mucoid ingesta. Additionally, a focal area of necrosis (~1 cm in diameter) was observed on the left lateral liver lobe.

Laboratory Results:
Blood smear prior to euthanasia demonstrated few neutrophils, mostly bands, with evidence of toxic change.

Microscopic Description:
The slide consists of multiple sections of small intestine. The villi are mildly blunted with occasional fusion. The epithelial cells are minimally to mildly hypertrophied and somewhat disorganized. Adhered to the surface and within the microvilli of the epithelial cells are moderate numbers of small, 2-4 micron diameter, basophilic, spherical protozoa. A separate population of protozoa is present within the lumen (numbers vary from section to section). These organisms are piriform to crescent-shaped, measure 5-7 microns in maximum dimension, and have two internal, parallel, oval, basophilic nuclei.

Contributor's Morphologic Diagnoses:
1. Small intestine, villus blunting and fusion, multifocal, mild with epithelial cell hypertrophy and dysplasia with intralesional protozoa (morphology consistent with *Cryptosporidium* sp.)

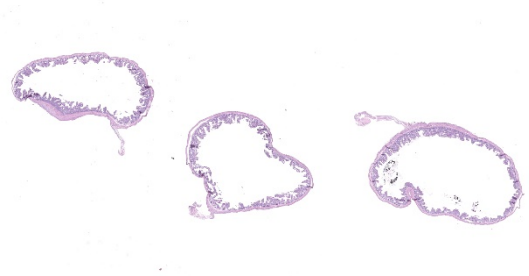

Figure 1-1. Jejunum, common marmoset. Three sections of jejunum are submitted for examination. There is diffuse blunting of villi. (HE, 6X)

2. Small intestine, intraluminal diplomanads, rare (morphology consistent with *Giardia* sp.)

Contributor's Comment:
This is a case of a concurrent infection of both *Giardia* sp. and *Cryptosporidium* sp. in a laboratory animal species and setting.

Cryptosporidium sp. are a group of zoonotic, protozoa of the phylum Apicomplexa. They are small, approximately 2-5 microns in diameter (depending on the life cycle stage) and are found on the epithelia of the gastrointestinal, respiratory, pancreatic, and biliary tracts of multiple animal species. There are many known species of *Cryptosporidium*, with some showing species specificity. The following are a few known species affecting domestic and exotic animal species: *C. parvum* in cattle, ruminants, and humans; *C. andersoni* in cattle; *C. suis* in pigs; *C. felis* in cats; *C. canis* in dogs; *C baileyi* and *C. meleagridis* in birds; and *C. serpentis* in reptiles.[4,12] Transmission of the protozoa is direct via fecal-oral route and often occurs due to contaminated drinking water as well as close contact with infected animals.[6] Pre-mortem diagnosis can be achieved by the rapid fecal antigen-capture ELISA or examining fresh feces microscopically.[9]

The life cycle of *Cryptosporidium* is similar to that of other apicomplexans.[4,12,14] After ingestion or inhalation of the oocyst stage, the sporozoites within the oocyst exit via excystation and adhere to mucosal epithelial cells. The sporozoites invade the cells and become surrounded by host cell membranes to form parasitophorous vacuoles. These vacuoles are often described as "extracytoplasmic" because they communicate with the host cell cytoplasm only via a feeder organelle. Within the parasitophorous vacuoles, the sporozoites develop into trophozoites, which then undergo asexual reproduction to form first generation meronts or schizonts that contain 4-8 merozoites. These merozoites are released into the lumen, which in turn infect additional epithelial cells. Merozoites then form second generation meronts (merogony) with additional merozoites, or undergo sexual reproduction and develop into gametes (gametogony). Male gametes are designated as microgamonts, and female gametes are known as macrogamonts. When combined, the gametes form an oocyst that then sporulates to contain four sporozoites. Once released, thin-walled sporocysts break down, released the sporozoites and allowing for autoinfection of the host. Thick-walled oocysts are passed in the feces.

Cryptosporidium sp. classically causes disease in immunocompromised animals and

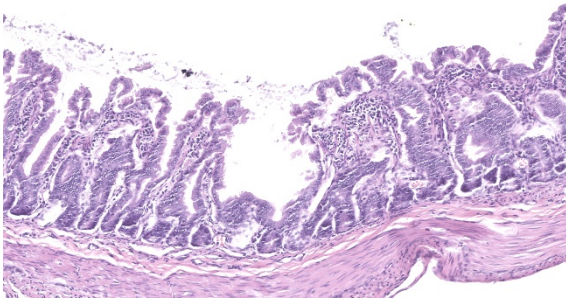

Figure 1-2. Jejunum, common marmoset. There is mild blunting of the villi (left), and villar fusion (right). (HE, 176X)

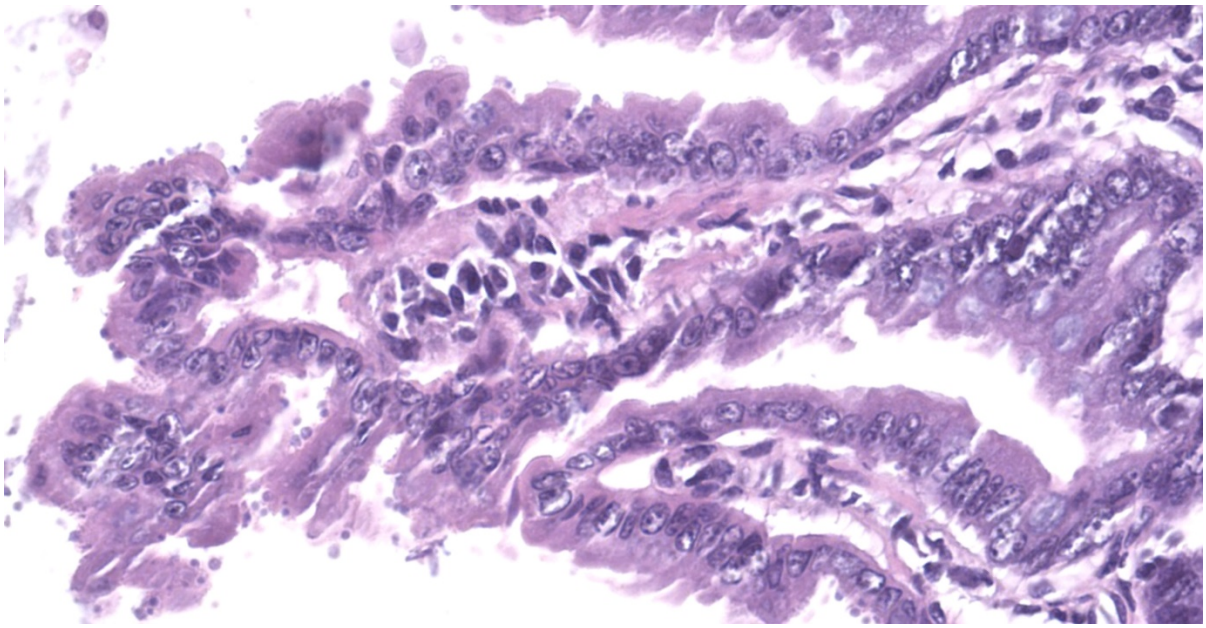

Figure 1-3. Jejunum, common marmoset. Cryptosporidial schizonts (smaller) and gamonts (larger) line the villar epithelium. (HE, 716X)

humans, particularly neonates and adults with underlying immunosuppressive diseases. In humans, *Cryptosporidium* is a very important zoonotic agent, typically affecting infants and young children as well as those with immunosuppressive conditions, most notably HIV.[2] Interestingly, disease in SIV-macaques has been reported to mimic an extraintestinal disease seen in HIV-infected patients.[8,13] In most animal species, especially young cattle, the protozoan generally causes a malabsorptive diarrhea of varying severity as a result of damage to the villi of enterocytes and, to a lesser extent, due to a reduction in overall absorptive surface area by the organisms themselves. Furthermore, the organism can incite a variable inflammatory response in the mucosa.[2] Infected marmosets may develop enterocolitis but usually remain subclinical.[9] Asymptomatic animals may become carriers and continue to intermittently shed the organism.

Giardia sp. are zoonotic, diplomonads that belong to the family Hexamitidae. They are typically found in the lumen of the small intestinal tract and are one of the more common flagellates of mammals and birds.[4] Unlike other members of the family (*Spironucleus, Trichomonas*), *Giardia* lack an undulating membrane – the trophozoite form contains two nuclei, two median bodies, two axonemes, and four pairs of flagella. Currently, there are six known species that infect a wide range of animal species: *G. agilis* in amphibians, *G. ardeae* and *G. pstittaci* in birds, *G. muris* and *G. microti* in rodents, and *G. duodenalis* in mammals.[10] Furthermore, *Giardia duodenalis* (a.k.a. *Giardia lamblia* or *Giardia intestinalis*) has several known, morphologically similar genotypes, each of which show some species specificity: assemblages A and B commonly infect humans; assemblages A and E infect hoofstock; assemblages C and D infect dogs; and assemblage F infects cats.[10]

The life cycle of *Giardia* sp. is rather simple in comparison to *Cryptosporidium*. There are two stages of the parasite: cyst and trophozoite.[4,12] The environmentally-resistant cyst is the infective form of the parasite, and is passed in the feces. Once ingested, excyzoites are released, and

transform into trophozoites, which then adhere to the microvilli of intestinal epithelial cells by an adhesive disk on the ventral surface of the organism.[16] The trophozoites will then replicate and encyst, followed by passage in the feces. Transmission is direct via fecal-oral route and, like *Cryptosporidium*, often occurs due to contaminated food and water sources. Diagnosis is typically made by demonstrating protozoal cysts in fecal floats or trophozoites in fecal or intestinal smears. Additionally, an ELISA and immunofluorescent staining of the cyst wall can be used for detection of the organism in feces.

Disease caused by *Giardia* is generally asymptomatic in humans and most animal species[6] and usually does not incite a significant host inflammatory response.[2] However, in young dogs and cats, Giardiasis is an important cause of chronic diarrhea. Moreover, *Giardia* is associated with enteric disease in neonatal calves, especially those with a poor growth rate. Infected marmosets do not usually show evidence of clinical disease, but will intermittently shed the organism.[9] Furthermore, Giardia may be a contributing factor to marmoset wasting syndrome.[7]

Contributing Institution:
Johns Hopkins University School of Medicine
Department of Molecular and Comparative Pathobiology
http://www.hopkinsmedicine.org/mcp

JPC Diagnosis:
1. Jejunum: Villar blunting and fusion, diffuse, mild to moderate with numerous intracellular apicomplexans, etiology consistent with *Cryptosporidium* sp.

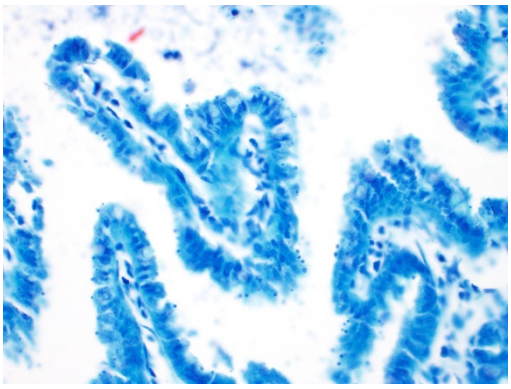

Figure 1-4. Jejunum, common marmoset. A Giemsa stain is useful for demonstrating cryptosporidia. (Giemsa, 400X)

2. Jejunum, lumen: Few extracellular flagellates, etiology consistent with *Giardia* sp.

3. Mesentery: Fat atrophy, diffuse, marked.

JPC Comment:
The contributor provides a thorough review of *Cryptosporidium* sp. and *Giardia* sp., two important zoonotic apicomplexan parasites encountered in many veterinary species.

Cryptosporidium sp. was first identified in laboratory mice by Tyzzer in 1907, but its role as a pathogen wasn't recognized until the 1970s when it was identified to cause disease in mammals, particularly calves. In immunocompetent mammalian hosts, cryptosporidiosis is generally a self-limiting disease. When infected, humans typically exhibit a 3-7 day incubation period followed by an acute onset of diarrhea and abdominal cramping with symptoms typically lasting 7-10 days. As noted by the contributor, cryptosporidiosis presents a serious risk to immunocompromised hosts and is one of the most serious opportunistic infections facing AIDs patients.[5]

Additional flagellates other than *Giardia* sp. that parasitize the intestinal tract include *Spironucleus* sp. and trichomonads. Each

have distinguishing characteristics, some of which are more apparent in tissue sections whereas others are best demonstrated in fresh fecal preparations. All are similar in size, with *Spironucleus* sp. being the smallest (5-12µm x 2-7µm trophozoites), followed by trichomonads (8-14µm trophozoites), and *Giardia* sp. being the largest (10-20µm x 5-15µm trophozoites with 10-14µm x 8-10µm cysts). In fresh fecal smears, *Spironucleus* sp. can be identified as small piriform flagellates that lack a sucking disk. Trichomonads are also characterized by a pear shape but are larger with a pointed posterior end from which a linear axostyle may protrude, a single nucleus, 3-5 anterior flagella, and an undulating membrane contiguous with the posterior flagellum. Trichomonad trophozoites are destroyed by floatation solutions but can be identified in preparations using saline. In tissue sections, *Giardia* sp. are often closely opposed to the mucosal epithelium with a ventrally flattened appearance due to the ventral adhesive disk, which is a specialized feature allowing for close association to the mucosal epithelium. In contrast, trichomonads have a rounder profile without ventral flattening in association with the small intestine mucosal epithelium, lack a cyst stage, have a single nucleus, and an undulating membrane.

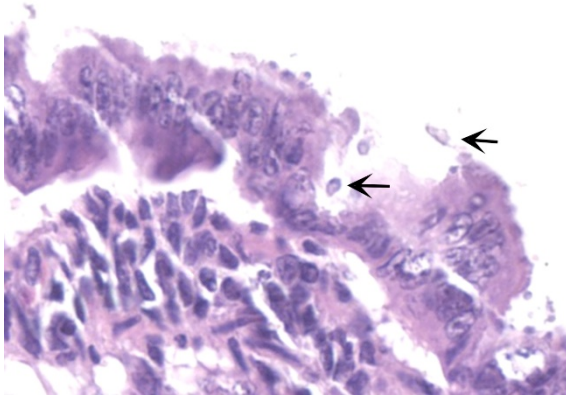

Figure 1-5. Jejunum, common marmoset. Rare pyriform Giardia are present within the lumen and adjacent to the mucosal epithelium. (HE, 716X)

Centrifugation floatation using 33% $ZnSO_4$ is preferred over fresh feces for the detection of *Giardia* sp. cysts. In addition, *Giardia* sp. trophozoites have a characteristic "falling leaf" or wobbling swimming motion in fresh fecal smears, which aids in distinguishing them from trichomonads.[11]

Although marmosets (*Callithrix* sp.) have a long history of being kept as pets, biomedical research saw a dramatic rise in their utilization following the establishment of the National Institutes of Health (NIH) primate centers program in the early 1960s. Multiple factors make these New World primates ideal models for biomedical research, including an approximately 93% sequence identity to the human genome (similar to macaques), small size (adults typically weight 300-450g), relatively short lifespan in comparison to other primates (13 years on average), and they are the most fertile of the primates, reaching sexual maturity by 1.5 years of age and produce litters of 2-3 offspring every 5-6 months. Marmosets are particularly well suited for cognition, behavior, and mental illness research studies given their shared functional brain architecture and behaviors with humans. Unlike Old World monkeys (OWM), marmosets have a lissencephalic (smooth) cortex, which greatly facilitates the recording and manipulation of brain activity in comparison to their OWM counterparts. Susceptible to a number of viruses, including hepatitis C, dengue, herpesvirus, SARS, Marburg, and Ebola, marmosets are ideal models for pharmacology and toxicology studies, especially since smaller amounts of test compounds are required due to their small body size. The most commonly used species is the common marmoset (*C. jacchus*), in addition to black-tufted and white-headed or Geoffroy's marmosets.[3]

One of the most significant problems facing captive marmoset colonies is 'wasting

marmoset syndrome' (WMS), which affects 28-60% of captive marmosets and is involved in 50-80% of deaths. Multiple reports state the primary disease of WMS is an inflammatory bowel disease (IBD) with chronic enteritis.[14] Common symptoms include weight loss, decreased muscle mass, alopecia (commonly at the tail base), and chronic diarrhea. One study found most marmosets weighing less than 325g were affected by WMS and 100% of affected marmosets suffered chronic weight loss of 0.05% of the peak body weight per day.[1]

Common bloodwork abnormalities associated with WMS include anemia, hyperproteinemia, hypoalbuminemia, and elevated serum alkaline phosphatase. However, postmortem examination is the gold standard for the diagnosis of WMS, with the hallmark lesion being chronic lymphoplasmacytic enterocolitis. The underlying cause of WMS is unknown with proposed etiologies including food allergies, parasitism, and autoimmune disease. WMS can significantly disrupt research studies and breeding programs as affected animals are often not identified until late in the disease process.[1]

One study found matrix metalloproteinase 9 (MMP9) serum levels are be significantly elevated in marmosets affected by WMS. This enzyme is thought to play a role in the pathogenesis of similar inflammatory conditions, including human and murine inflammatory bowel disease, by degrading extracellular matrix components. Therefore MMP9 may not only be useful as a biomarker for WMS diagnosis but also as a target of therapeutic intervention.[13] A more recent study found marmosets with WMS treated with transexamic acid, in combination with amino acid and iron supplementation, to have reduced serum MMP9 levels, ameliorated alopecia, and increased body weight and hematocrit. These animals continued to gain or maintain body weight for at least three months following the experiment. Transexmanic acid suppresses MMP9 by inhibiting its activator, plasmin.[15]

References:

1. Baxter VK, Shaw GC, Sotuyo NP, et al. Serum albumin and body weight as biomarkers for the antemortem identification of bone and gastrointestinal disease in the common marmoset. *PLoS One*. 2013;8(12):e82747.
2. Certad G, Viscogliosi E, Chabe M, Caccio SM. Pathogenic mechanisms of Cryptosporidium and Giardia. Trends Parasitol. 2017. (Epub ahead of print).
3. Colman RJ, Capuano S, Bakker J, Keeley J, Nakamura K, Ross C. Marmosets: Welfare, Ethical Use, and IACUC/Regulatory Considerations [published online ahead of print, 2021 Feb 23]. *ILAR J*. 2021;ilab003.
4. Gardiner CH, Fayer R, Dubey JP. An Atlas of Protozoan Parasites in Animal Tissues. 2nd ed. Washington, DC: Armed Forces Institute of Pathology; 1984:6-7, 37-39.
5. Hahn NE, Capuano SV 3rd. Successful treatment of cryptosporidiosis in 2 common marmosets (Callithrix jacchus) by using paromomycin. *J Am Assoc Lab Anim Sci*. 2010;49(6):873-875.
6. Johnson-Delaney CA. Parasites of captive nonhuman primates. Vet Clin Exot Anim. 2009;12(3):563-581.
7. Kramer JA, Hachey AM, Wachtman LM Mansfield KG. Treatment of Giardiasis in common marmosets (Callithrix jacchus) with Tinidazole. Comp Med. 2009;59(2): 174-179.
8. Kvac M, McEnvoy J, Stenger B, Clark M. Cryptosporidiosis in other vertebrates. In: Caccio SM and Widmer G, ed. Cryptosporidium: parasite and disease. New York: Springer; 2014: 237-323.

9. Ludlage E, Mansfield K. Clinical care and diseases of the common marmoset (Callithrix jacchus). Comp Med. 2003;53(4):369-382.
10. Ryan U, Caccio SM. Zoonotic potential of Giardia. Int J Parasitol. 2013;43:943-956.
11. Sheppard BJ, Stockdale Walden HD, Kondo H. Syrian hamsters (Mesocricetus auratus) with simultaneous intestinal Giardia sp., Spironucleus sp., and trichomonad infections. *J Vet Diagn Invest*. 2013;25(6):785-790.
12. Uzal FA, Plattner BL, Hostetter JM. Alimentary System. In: Maxie MG, ed. Pathology of Domestic Animals. 6th ed. St. Louis, MO: Elsevier; 2016:293-243.
13. Yanai T, Chalifoux LV, Mansfield KG, Lackner AA, Simon MA. Pulmonary Cryptosporidiosis in Simian immunodeficiency virus-infected Rhesus Macaques. Vet Pathol. 2000;37(5):472-475.
14. Yoshimoto T, Niimi K, Takahashi E. Serum matrix metalloproteinase 9 (MMP9) as a biochemical marker for wasting marmoset syndrome. *J Vet Med Sci*. 2016;78(5):837-843.
15. Yoshimoto T, Niimi K, Takahashi E. Tranexamic Acid and Supportive Measures to Treat Wasting Marmoset Syndrome. *Comp Med*. 2016;66(6):468-473.
16. Zachary JF. Protozoan diseases of organ systems. In: Zachary JF, ed. Pathologic Basis of Veterinary Disease. 6th ed. St. Louis, MO: Elsevier; 2017:236-238.

CASE II:

Signalment:
11-years-old**,** female, Miniature schnauzer, dog (*Canis familiaris*)

History:
The dog presented with subcutaneous mass in left submandibular area. The mass was resected, and submitted to pathological examination.

Gross Pathology:
The mass was solid. The cut surface of the mass was solid and firm, and brown-gray in color. The mass was considered as the mandibular gland because of the location adjacent to the parotid gland.

Laboratory Results:
No laboratory findings reported.

Microscopic Description:
Extensive coagulative necrosis of the mandibular gland was observed with presentation of the lobular architecture. There was thrombosis of small and large vessels in the necrotic areas. The affected lobule of the mandibular gland was surrounded by thick fibrous capsule. In the peripheral area of lobule beneath fibrous capsule, there was ductal hyperplasia and squamous metaplasia of ductal epithelium with edema, hemorrhage and inflammatory cell infiltration. The hyperplastic ducts sometimes reached to lobular capsule. Ductal epithelium had vesicular nuclei with mild anisokaryosis and small number of mitoses, but no plemorphism or atypia. Hyperplastic ducts were lined by basement membranes and did not show any invasion to surrounding tissues. In the parotid gland adjacent to the mandibular gland, there was slight enlargement of ducts, however no necrosis or other histological abnormalities were found.

Contributor's Morphologic Diagnoses:
Necrotizing sialometaplasia.

Contributor's Comment:
Necrotizing sialometaplasia (NS) is rarely reported in animals, although naturally occurring cases have been reported in dogs and cats, in addition to one spontaneous case in rabbit and one experimentally induced case in a rat.[1,3,5,7] NS has been reported to account for 6% (9/160) of canine salivary gland diseases and most cases were seen in small breed dogs, primarily terriers. NS most commonly affects the mandibular gland in dogs, although the parotid salivary gland was reported to be affected in one case.[3,5] Any salivary gland may be affected in humans; most cases have been reported in the oral cavity, commonly at the junction of hard and soft plates.[9]

The exact etiology and pathogenesis NS is not known. The causes are thought to be vascular injury, type III hypersensitivity, *Bartonella spp.* infection, or immune mediated vasculitis.[3,5,7] The most widely accepted theory explaining the etiology of NS is injury of the blood vessels, leading to ischemic and infarction of the salivary gland acini. It is unclear if the dog in this case had traumatic vascular injury, as vasculitis is not observed in the examined tissue sections.

The main histological features of NS observed in this case include extensive coagulative necrosis of salivary tissue, vasculopathy including vascular thrombosis and/or fibrinoid degeneration, squamous metaplasia of ducts and acini, and variable inflammation and fibrosis. These features are easily and often misinterpreted as malignant transformation. Hyperplastic ductal elements and squamous metaplasia are often mistaken for squamous cell carcinoma. Some characteristics used to distinguish NS from squamous cell carcinoma include presser-vation of the general lobular structure of salivary gland and absence of atypical nuclei in the metaplastic squamous epithelium.

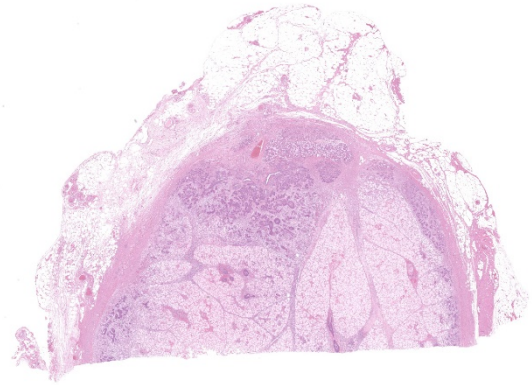

Figure 2-1. Submandibular salivary gland, dog. A section of a bisected salivary gland is presented for examination. Several lobules are necrotic and have lost stain affinity (lower right). There is ductal proliferation at top center. (HE, 6X)

Fibrinoid necrosis of arteries was not observed on our case, however, the histological features were identical to the characteristics of NS and sufficient to diagnose as NS.

Contributing Institution:
Laboratory of Pathology, Faculty of Pharmaceutical Sciences, Setsunan University,
45-1 Nagaotohge-cho, Hirakata, Osaka 573-0101, Japan

JPC Diagnosis:
Salivary gland, submandibular: Coagulative necrosis (infarct), focally extensive, with ductular degeneration, necrosis, and regeneration, and acinar atrophy.

JPC Comment:
The contributor provides a concise review of a unique lesion frequently mistaken for a neoplastic process by neophyte pathologists. A recent retrospective study of salivary gland diseases in 179 dogs found only 2.2% of salivary glands submitted to be consistent with necrotizing sialometaplasia. In contrast, the most common diagnosis was non-specific

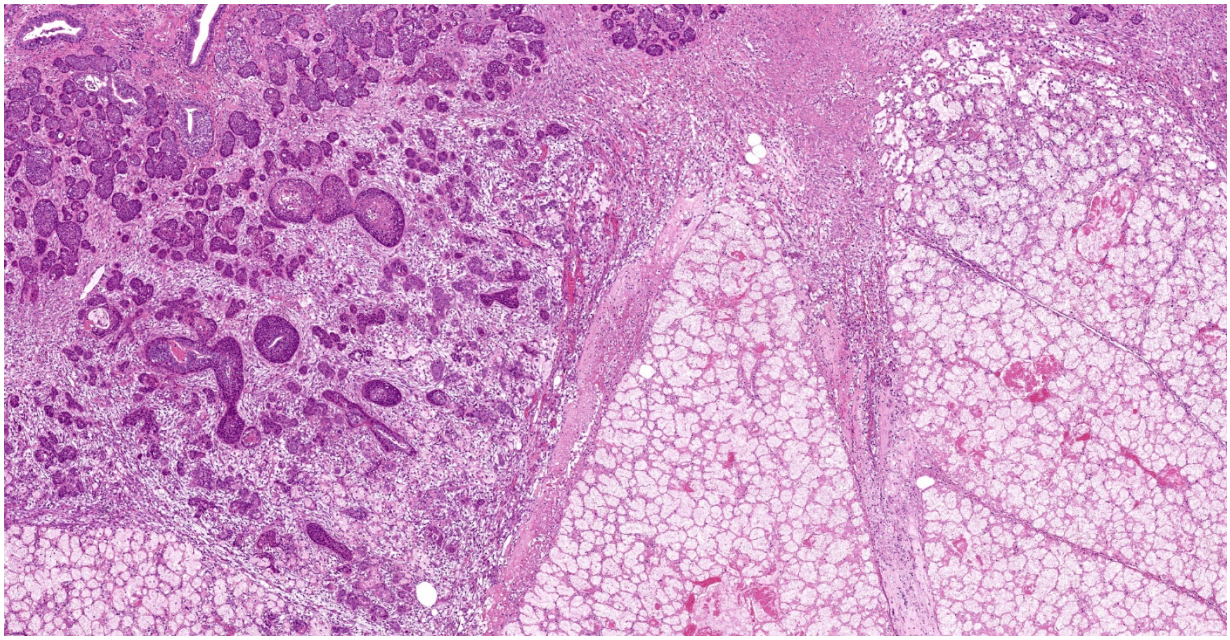

Figure 2-2. Submandibular salivary gland, dog. The lobule at right is infarcted. The lobule at left is effaced by granulation tissue and proliferating regenerating salivary ducts. (HE, 35X)

sialoadenitis(20.1%), and lipomatosis (3.9%). Nearly 70% of the lesions noted in this case series affected a major extraoral salivary gland, with the mandibular salivary gland being the most common.[4]

In regard to neoplastic disease, 88.8% of neoplasms were epithelial, followed by round cell (5.5%), carcinosarcoma (2.7%), and undetermined (2.7%). Of the 36 epithelial neoplasms, the most common type was adenocarcinoma (14/36), followed by mucoepidermoid carcinoma (10/36), acinic cell carcinoma (7/36), and squamous cell carcinoma (1/36). Lipomatosis was characterized by widespread expansion of salivary glands by adipocytes with secondary lobular atrophy.[4]

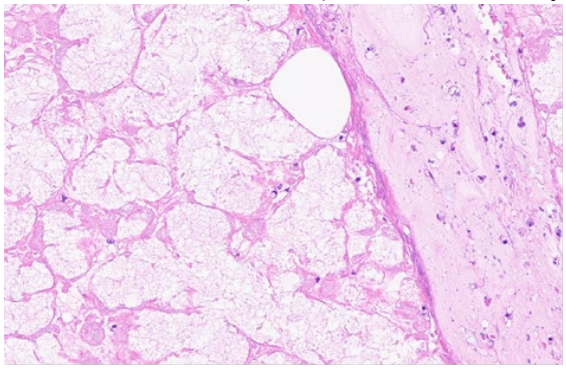

Figure 2-3. Submandibular salivary gland, dog. Higher magnification of the infarcted lobules and edematous interlobular septa. (HE, 164X)

Patients affected by necrotizing sialometaplasia may present with mild to severe clinical signs. Mild cases are typically characterized by unilateral swelling of the affected salivary gland with occasional pyrexia and anorexia. These cases typically resolve within 10 days regardless of medical intervention. In contrast, severe cases manifest with extreme pain, nausea, dysphagia, anorexia, gagging, and vomiting. These cases are rare and nearly always affect young small terrier breeds. Unfortunately, excision of the affected gland is not curative in these severe cases and euthanasia is often elected due to intractable pain and vomiting.

Although both the mild and severe forms have identical histologic features, some authors suggest using the term "salivary gland infarction" to define patients with clinical signs consistent with the mild form of the disease whereas "necrotizing sialometaplasia" should be reserved for small terrier breeds demonstrating severe clinical signs.[6]

As noted by the contributor, necrotizing sialometaplasia in histologic sections is characterized by extensive, well-demarcated areas of coagulative necrosis bordered by mixed inflammatory cells and fibrosis, vascular thrombosis, and hyperplastic ducts with squamous metaplasia. Necrotizing sialometaplasia can closely resemble salivary gland carcinoma or squamous cell carcinoma, particularly if only small tissue sections are examined. However, key distinguishing features consistent with necrotizing sialometaplasia include extensive, well-demarcated regions of infarction with normal adjacent salivary gland tissue with a lack of solid acinar proliferation.[4]

Humans are similarly affected by necrotizing sialometaplasia, though the distribution differs from those described in companion animals. In humans, necrotizing sialometaplasia most commonly affects the minor salivary glands of the hard palate whereas the mandibular salivary gland is most commonly affected in canines and felines. As in veterinary species, the underlying pathogenesis is unclear but the disease is believed to occur due to ischemia of the salivary gland lobules with subsequent infarction. Potential causes of ischemia identified in humans include direct trauma, alcohol and cocaine use, radiation, administration local anesthetics with vasoconstriction agents, surgical procedures, tobacco products, and bulimia. In humans, immunohisochemical

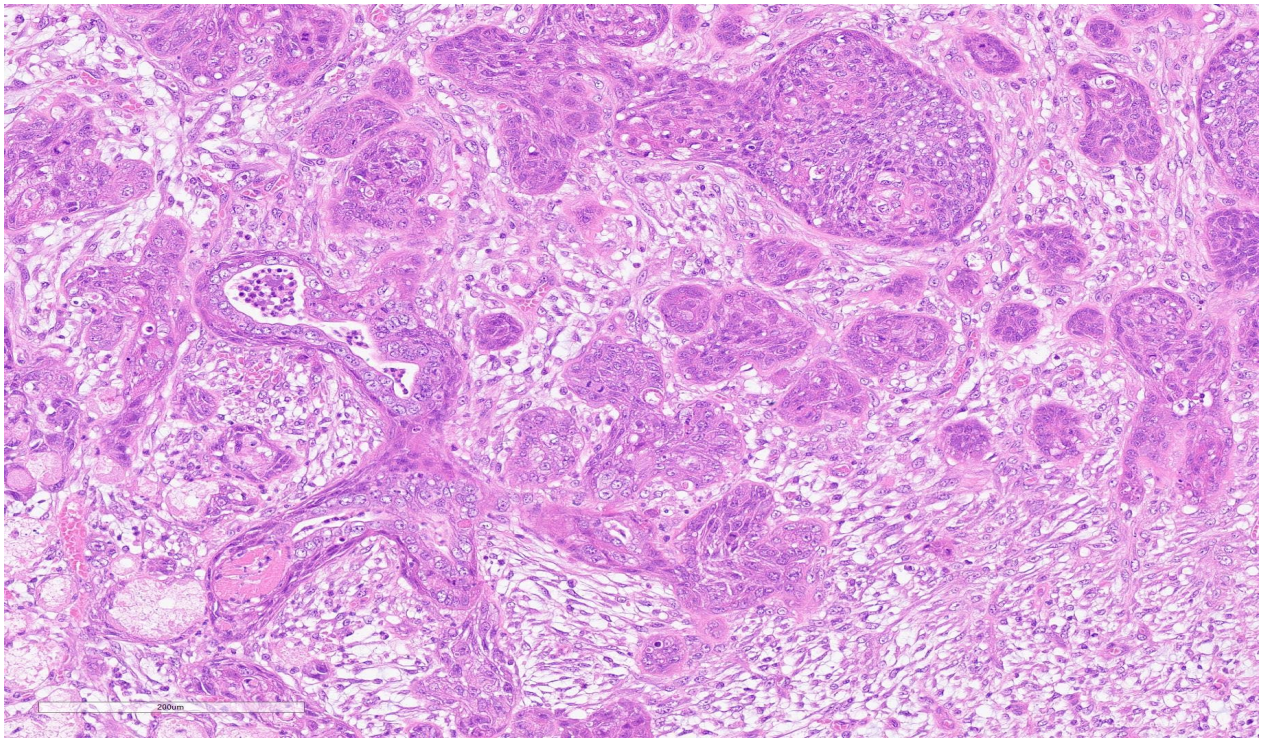

Figure 2-4. Submandibular salivary gland, dog. Higher magnification of the ductal regeneration. Lining epithelium is hyperplastic and hypertrophic. Ducts with lumina contain moderate numbers of neutrophils. (HE, 226X)

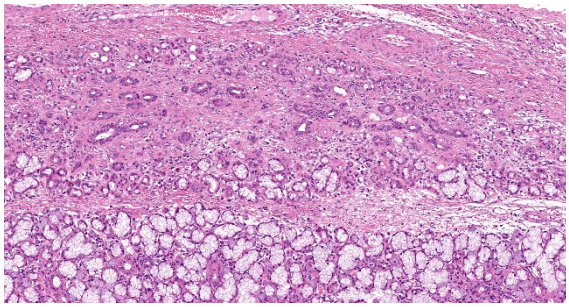

Figure 2-5. Submandibular salivary gland, dog. Some lobules are fibrotic, with ductal regeneration apposing acinar atrophy. (HE, 115X)

stains for cytokeratin 7 (CK7) and α-smooth muscle actin are often used to definitively differentiate necrotizing sialometaplasia from neoplastic disease. Squamous cells associated with necrotizing sialometaplasia are commonly immunopositive for CK7 while most squamous cell carcinomas are not. In cases of necrotizing squamous metaplasia, islands of epithelial cells are typically surrounded by a residual layer of myoepithelial cells immunoreactive to α-smooth muscle actin whereas most squamous cell carcinomas and mucoepidermoid carcinomas are negative.[2]

References:

1. Brown PJ, Bradshaw JM, Sozmen M, Campbell RH: Feline necrotising sialometaplasia: a report of two cases. *J Feline Med Surg* 2004:6(4)**:**279-281.
2. Chateaubriand SL, de Amorim Carvalho EJ, Leite AA, da Silva Leonel ACL, Prado JD, da Cruz Perez DE. Necrotizing sialometaplasia: A diagnostic challenge. *Oral Oncol*. 2021;118:105349.
3. Kim HY, Woo GH, Bae YC, Park YH, Joo YS: Necrotizing sialometaplasia of the parotid gland in a dog. *J Vet Diagn Invest* 2010:22(6)**:**975-977.
4. Lieske DE, Rissi DR. A retrospective study of salivary gland diseases in 179 dogs (2010-2018). *J Vet Diagn Invest*. 2020;32(4):604-610.
5. Mukaratirwa S, Petterino C, Bradley A: Spontaneous necrotizing sialometaplasia of the submandibular salivary gland in a Beagle dog. *J Toxicol Pathol* 2015:28(3)**:**177-180.
6. Munday JS, Lohr CV, Kiupel M. Tumors of the alimentary tract. In: Meuten DJ, ed. *Tumors in Domestic Animals*. 5th ed. Ames, Iowa: Iowa State Press; 2017:548.
7. Saunders GK, Monroe WE: Systemic granulomatous disease and sialometaplasia in a dog with Bartonella infection. *Vet Pathol* 2006:43(3)**:**391-392.
8. Villano JS, Cooper TK: Mandibular fracture and necrotizing sialometaplasia in a rabbit. *Comp Med* 2013:63(1)**:**67-70.
9. Ylikontiola L, Siponen M, Salo T, Sandor GK: Sialometaplasia of the soft palate in a 2-year-old girl. *J Can Dent Assoc* 2007:73(4)**:**333-336.

CASE III:

Signalment:
Male NSG (NOD.*Cg-Prkdc*^{scid}*Il2rg*^{tm1Wjl}/SzJ) mouse. Age unknown.

History:
The colony was recently treated with trimethoprim sulfamethoxazole for an outbreak of diarrhea. Several animals have been found dead or presented moribund.

Gross Pathology:
The mouse was in poor body condition with scant amounts of visceral fat. The left cranial lung lobe was effaced by a 1 X 0.8 X 0.8 cm mass (abscess) containing some white to yellow/green material (pus), with multifocal nodules throughout the rest of the left lung. Right lung was not affected.

Laboratory Results:
Bacterial culture of the lungs returned *Klebsiella pneumoniae* (string test negative).

Microscopic Description:
Lung: The submitted lung section consists of a large expansile abscess that severely effaces the pulmonary parenchymal architecture as well as multiple discrete foci of severely distended bronchioles plugged with basophilic necropurulent and proteinaceous exudative material. The abscess is composed of large core of necrotic and proteinaceous material surrounded by massive numbers degenerate neutrophils, karyorrhectic debris, basophilic lytic chromatin and mineralized material admixed with multifocal aggregates of intralesional bacilli. The periphery of the abscess is composed of a variable thick band of collagen fibers admixed with hypertrophic stromal cells, numerous large foamy macrophages and abundant neovascularization. The affected bronchioles, are filled with basophilic concretions of large numbers of degenerate neutrophils, ghost cells, karyorrhectic debris, fibrin deposition, aggregates of bacilli, with few dispersed, eosinophilic, linear to rhomboid crystalline material. There is also marked attenuation of bronchiolar epithelium or loss of epithelium lining. There is expansion and splitting of the bronchial walls by edema and associated inflammation. Most of the alveoli between these dilated bronchioles are filled with aggregates of degenerate neutrophils, proteinaceous material along with prominent alveolar septal necrosis, type II pneumocyte hyperplasia, edema, vascular congestion, and mild hemorrhage. In less affected areas, the alveolar space is occupied by a few foamy macrophages, and multinucleated giant cells are also rarely noted.

Contributor's Morphologic Diagnoses:
1. Lung: Severe, multifocal to coalescing, acute, necrotizing fibrinosuppurative bronchopneumonia, with pulmonary abscessation, septal necrosis, type II pneumocyte hyperplasia, pulmonary edema, congestion, and intralesional bacilli.

2. Mild, multifocal, chronic, histiocytic pneumonia, with intraalveolar eosinophilic crystals, lung, mouse.

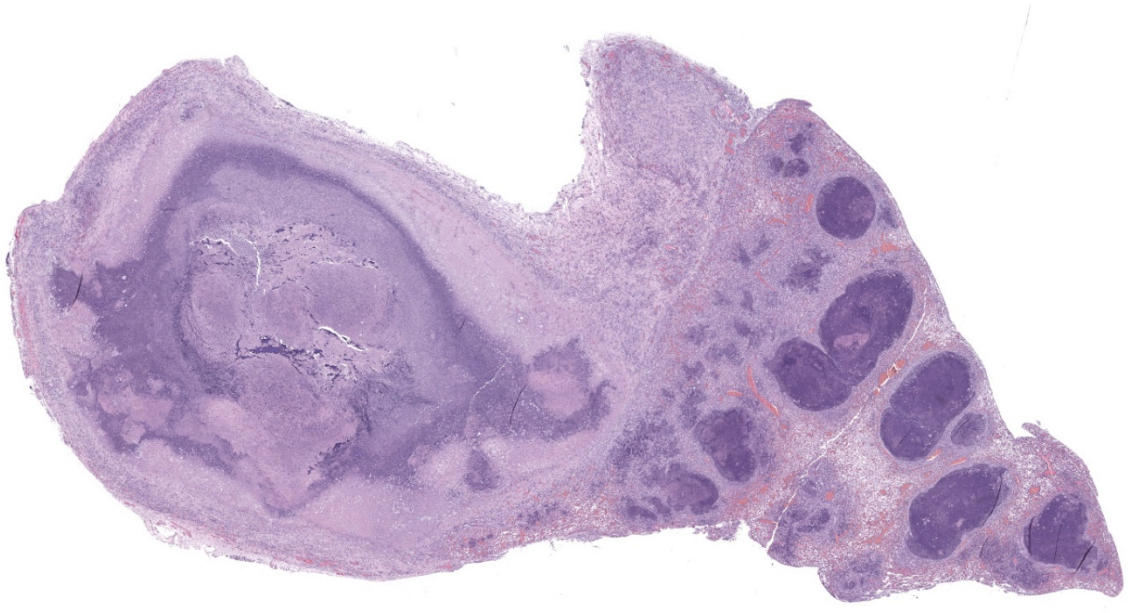

Figure 3-1. Lung, mouse: Large areas of the lung are replaced by an abscess (left) and lytic necrosis which are centered on airways. (HE, 5X)

Contributor's Comment:

This case presents a classic *Klebsiella pneumoniae* lesion: bacterial pneumonia with extensive lytic necrosis.[1] This mouse also had a severe multifocal fibrinosuppurative meningitis (not shown), a lesion commonly seen in human patients.[6] *Klebsiella pneumoniae* is a common commensal bacterial species found in the gastrointestinal tract of healthy mice, but can be an opportunistic pathogen especially for immunocompromised mice.[6] In recent years the emergence of hypervirulent strains, characterized by their thick capsule which produces a hyperviscomucoid phenotype (as identified using the "string test") have emerged as important pathogen in nosocomial and community acquired infections in humans.[8] The strains of *Klebsiella pneumoniae* isolated from this colony of the present case were overwhelmingly "classical" or non-hypervirulent.

The presented mouse came from a colony, which were previously treated with TMP/SMX for an outbreak of diarrhea; many of the *Klebsiella pneumoniae* strains isolated from this colony were resistant to this antibiotic; *Klebsiella pneumoniae* commonly contain multiple antibiotic resistance genes.[7] While it is unclear in this case what role the antibiotic treatment played, it is well established that antibiotic induced dysbiosis can allow the overgrowth of normal microbiome species, leading to disease.[1] This mouse, along with several in this room, also had a high burden of trichomonads, later confirmed on PCR to be *Tritrichomonas muris*. These organisms are normally thought of as non-pathogenic and was considered an incidental finding.[1]

NSG (NOD.*Cg-Prkdc*^{scid}*Il2rg*^{tm1Wjl}/SzJ) mice contain several critical mutations (NOD/ShiLtJ background with severe combined immune deficiency mutation (scid)

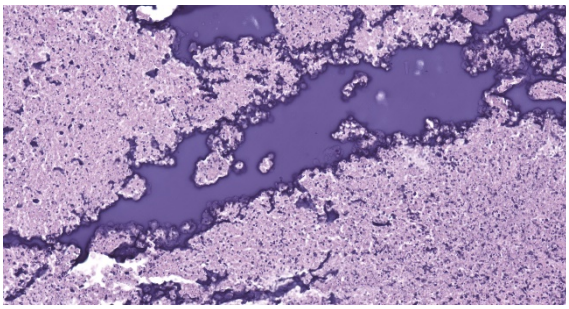

Figure 3-2. Lung, mouse. Within the abscess, admixed with cellular debris, are large aggregates of deeply basophilic nuclear protein (HE, 335X)

and an interleukin-2 (IL-2) receptor gamma chain deficiency). These mice do not have functional T and B cells, NK cells, and hemolytic complement; they lack cytokine signaling due to deficiency of IL-2 gamma chain as the common receptor.[3] Because of profound immunodeficiency, NSG mice have been widely used for research of xenotransplantation, serving as "humanized mice".[3] Severe immunocompromised condition also put NSG mice in high risk of opportunistic bacterial infections. A report has revealed that spontaneous mortality had occurred in NSG mice, and 10-20% of mortality was caused by nephritis associated with *Enterococcus* sp. or *Klebsiella oxytoca*, both of which were opportunistic pathogens.[3] Previously, there have been case reports with thorough reviews regarding *Klebsiella* pneumonia in CyBB knockout mouse (Mus musculus, JPC 4101147) and *Klebsiella*-induced meningoencephalitis in NSG mouse (Mus musculus, JPC 4128009). This case will be a great comparison for previous cases.

In humans, the *K. pneumoniae* infection could turn into serious nosocomial diseases, also known as *Klebsiella*-associated syndromes (KAS). The pathological manifestations are liver abscesses, pneumonia, and bacteremia, potentially meningoencephalitis and endophthalmitis.[2,5] In non-human primates, *K. pneumoniae* infection is not common. A study in 2020[5]

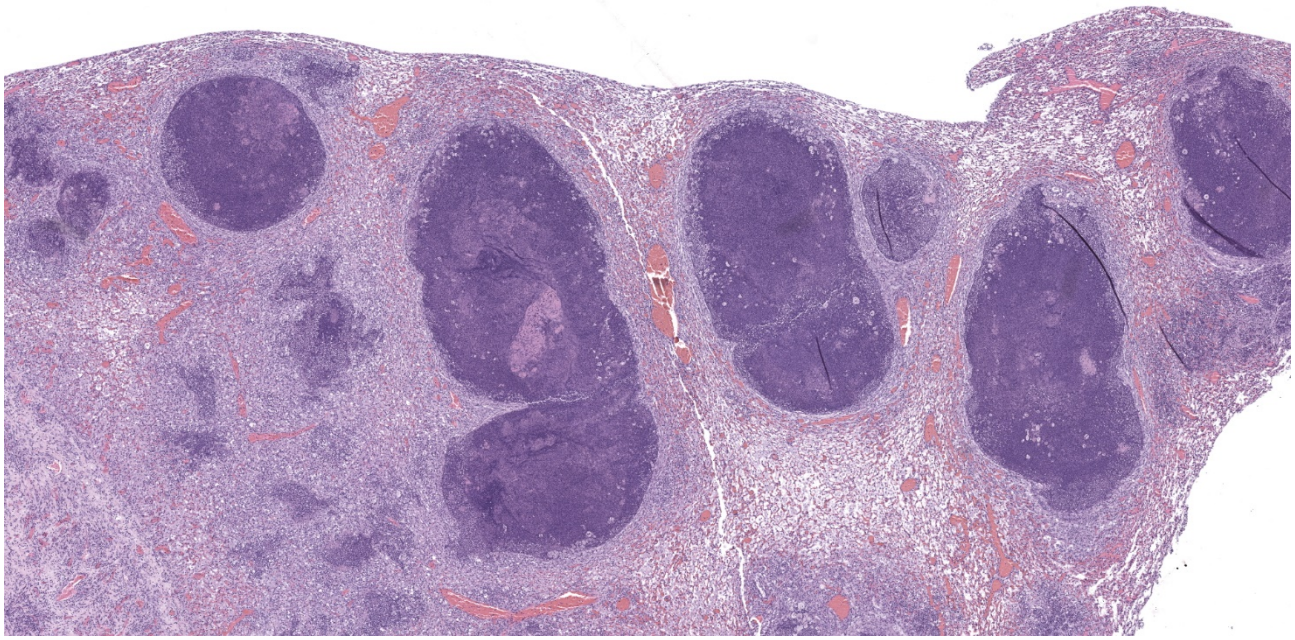

Figure 3-3. Lung, mouse. In the other half of the lung, airways are expanded by large numbers of necrotic neutrophils and cellular debris. (HE, 27X)

revealed that a total number of 9 predominantly outdoor-housed rhesus macaques (*Macaca mulatta*) presented for pneumonia (n=6), meningoencephalitis (n=7), endophthalmitis/optic neuritis (n=3), liver abscess (n=2), and other nonspecific findings such as gastric rupture (n=1), endometriosis (n=1), amyloidosis in liver/kidneys/intestines (n=2), thyroid tumor (n=1), and colonic adenocarcinoma (n=1). These animals tested positive for *K. pneumonia* through PCR or bacterial culture, from tissues of lung, brain, bone marrow, pleura, and peritoneum.[5] Another study showed that 7 African green monkeys (*Chlorocebus aethiops*) presented multi-systemic abscesses in abdominal cavity or in lungs, with positive bacterial culture of *K. pneumonia* with a hyperviscous mucoid phenotype in the string test.[10]

There are very few case reports of *K. pneumonia* in other animal species. A case report revealed 7 California Sea Lions (*Zalophus californianus*) presented with severe purulent bronchopneumonia, fibrinonecrotizing pleuritis, and pyothorax, and infection of hypervirulent (hypervis-comucoid) strain of *K. pneumoniae* was confirmed through serotyping, PCR, sequencing, and immunohistochemistry.[9]

Klebsiella pneumonia posted a zoonotic potential, since the bacteria shares the common molecular/phenotypes between humans and animals.[11] Eosinophilic crystalline pneumonia, also known as acidophilic macrophage pneumonia (AMP), is a common background lesion in lab animals. The eosinophilic crystals are composed of Ym1 and Ym2 chitinase, with iron, alpha-1 antitrypsin, immunoglobulin, and fragments of granulocytes.[4]

Contributing Institution:
The Division of Comparative Medicine, Massachusetts Institute of Technology
https://comp-med.mit.edu/

JPC Diagnosis:
Lung: Bronchopneumonia, necro-suppurative, multifocal to coalescing, severe, with abscessation.

JPC Comment:
The contributor provides an excellent review of manifestations of *Klebsiella* sp. infection reported in various species.

Klebsiella pneumoniae is a gram-negative, non-motile, encapsulated, facultative anaerobic, non-spore forming, non-flagellated, bacillus in the *Enterobacteriaceae* family. *K. pneumoniae* has numerous virulence factors, including (but not limited to) its capsule, lipopolysaccharide (LPS), siderophores, and fimbriae (also known as pili).

The capsule is composed of an extracellular polysaccharide matrix that surrounds the bacteria. Classic strains of *K. pneumoniae* produce capsules with serotypes K1 to K78, with K1 and K2 being more pathogenic. Highly virulent (HV) strains amplify the production of capsular material, resulting in a hypercapsule, and are predominately of the K1 serotype with fewer in the K2 serotype. The capsule significantly contributes to *K. pneumoniae*'s pathogenesis by inhibiting phagocytosis, hindering the bactericidal action of antimicrobial peptides such as β-defensins and lactoferin, preventing complement-mediated lysis and opsonization by blocking the binding of complement (e.g. C3), and downregulates the immune response by decreasing reactive oxygen species, IL-8, IL-6, and TNF-α production via activating a NOD-dependant pathway and shielding LPS recognition by TLR receptors. Enhanced capsule production may occur in HV strains in multiple ways, including expression of mucoid phenotype A (*rmpA*) and *rmpB* as plasmid-borne transcription regulators, chromosomal expression of *rmpA*, and regulation of the capsule synthesis A and B genes (*rcsA* and *rcsB*). In addition, hypercaspule production may also be initiated independantly by the chromosomal mucoviscosity-associated gene A (*magA*), which is restricted to K1 strains.[8]

LPS is a component of gram-negative bacteria and is composed of three major components: lipid A, an oligosaccharide core, and O antigen. Lipid A is connected to the bacteria's membrane and is a well-known pathogen associated molecular pattern recognized by TLR4. TLR4 activation leads to the recruitment of neutrophils and macrophages via production of cytokines and chemokines. However, multiple strains of *K. pneumoniae* evade TLR4 activation through various mechanisms, including masking of LPS with the capsule (K1, K10, and K16 strains), dampening TLR4 signaling using the capsule, or potentially modify LPS

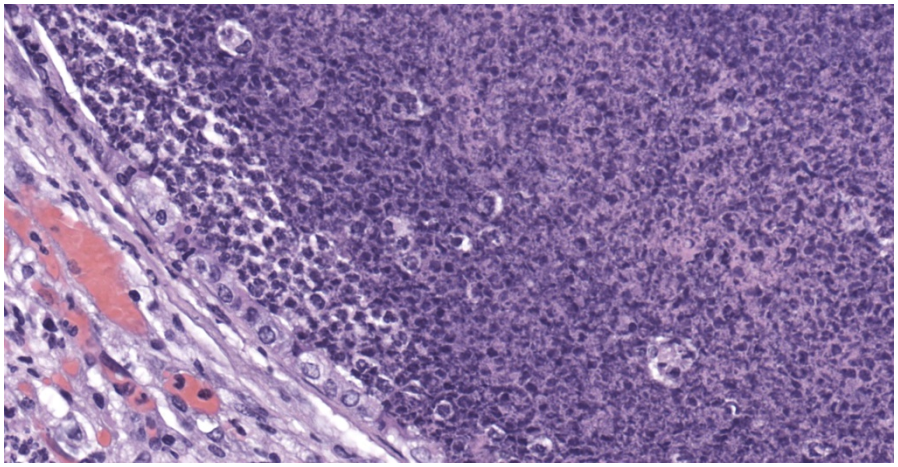

Figure 3-4. Lung, mouse. Areas of lytic necrosis are partially to circumferentially bound by cuboidal airway epithelium, demonstrating that they arise in airways. (HE, 27X)

into a no longer recognizable form. LPS remodeling has been reported to occur in other bacteria such as *Yersinia pestis* and *Helicobacter pylori.*[7]

The O antigen of LPS also protects the bacterium from complement mediated destruction. Although *K. penumoniae* is recognized by the classical, alternative, and lectin complement pathways, strains with the full length O antigen (or "smooth LPS") are protected from the effects the membrane attack complex by binding complement (i.e. C3b) far away from the cell membrane, rendering the membrane attack complex ineffective. Strains with a truncated or absent O antigen (or "rough LPS") are more susceptible to killing via the classical complement pathway due to the increased ability for C1q to bind to the cell's surface.[8]

Fimbriae are a common feature of almost all members of *Enterobacteriaceae*, including *K. pneumoniae*, which has both type 1 and type 3 fimbriae. Type 1 fimbriae are composed of FimA subunits with the FimH subunit at the tip. These filamentous, membrane-bound, adhesive structures facilitate *K.* pneumoniae's ability to colonize the urinary tract in addition to biofilm formation. However, type 1 fimbriae are also immunogenic, as they amplify lectinophagocytosis by macrophages and neutrophils while the FimH subunit also binds to mast cells, resulting in increased immune cell activation and recruitment of neutrophils. Interestingly, *K. pneumoniae* appears to regulate the expression of type 1 fimbriae genes as they're expressed within the urinary tract but not in the gastrointestinal tract or lungs. Type 3 fimbriae are helix-like, membrane bound, adhesive structures that are notably required for the formation of biofilm production and adhesion on medical devices such as endotracheal tubes, giving the bacteria access to the lungs.[8]

The fourth major virulence factor utilized by *K. pneumoniae* is its use of siderophores to scavenge iron from the host. As with many bacteria, the pathogen requires iron in order to thrive, which correlates to iron sequestration by the host as a component of the innate immune response. Under normal conditions, iron is typically bound to transport molecules such as transferrin; however, mammalian species shift iron to lactoferrin, an innate defense protein, during bacterial infections. Siderophores possess higher affinities for iron than host transport proteins and also have

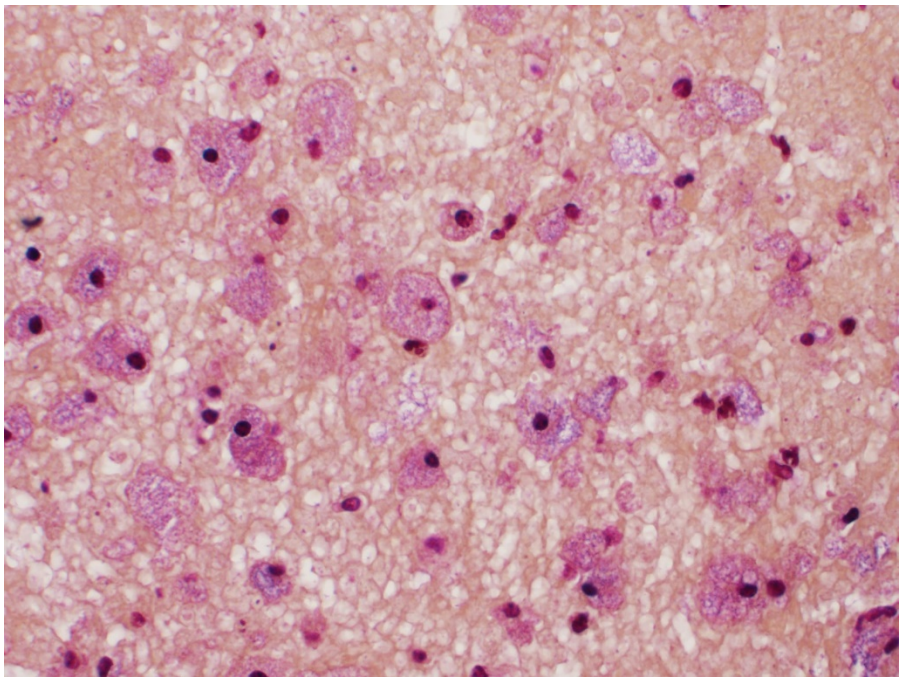

Figure 3-5. Lung, mouse. A Brown-Hopps Gram stain demonstrates small bacilli within macrophages. (BH, 600X)

the ability to liberate iron from chelating proteins while also scavenging iron from the environment. *K. pneumonia* has been found to produce one or more of the following siderophores: enterobactin aerobactin, salmochelin, and yersiniabactin. Nearly all classical and HV strains of *K. pneumoniae* produce enterobactin, which is considered to the primary iron uptake system utilized by this species.[8]

K. pneumoniae possesses many additional virulence factors, including outer membrane proteins (OMPs), porins, efflux pumps, and transporters, which in combination with the previously described factors impart a high level of resiliency to this pathogen, making it particularly well suited to resist both host immune defenses as well as therapeutic intervention.[8]

Conference attendees discussed the significance of eosinophilic crystals consistent with acidophilic macrophage pneumonia (MAP). It is unclear if MAP is simply a background lesion or developed secondary to the severe bronchopneumonia observed in this case. In addition, most participants noted bacteria consistent with *K. pneumoniae* were inapparent in their sections, highlighting the importance of bacterial culture in regard to the determination of an etiologic diagnosis in similar cases.

References:

1. Barthold, S., Griffey, S., Percy D. *Pathology of Laboratory Rodents and Rabbits, Fourth Edition*. Chichester: John Wiley & Sons, Inc.; 2016.
2. Büyüktuna SA, Hasbek M, Çelik C, et al. Yoğun Bakım Ünitesinde Gelişen Klebsiella pneumoniae Enfeksiyonları: Karbapenem Direnci ve Hasta Mortalitesi ile İlgili Risk Faktörler. *Mikrobiyol Bul*. 2020 15;54:378–391.
3. Foreman O, Kavirayani AM, Griffey SM, Reader R, Shultz LD. Opportunistic Bacterial Infections in Breeding Colonies of the NSG Mouse Strain. *Vet Pathol*. 2011 3;48:495–499.
4. Hoenerhoff MJ, Starost MF, Ward JM. Eosinophilic crystalline pneumonia as a major cause of death in 129S4/SvJae mice. *Vet Pathol*. 2006 Sep;43(5):682-8
5. Keesler RI, Colagross-Schouten A, Reader JR. Clinical and Pathologic Features of Spontaneous Klebsiella pneumoniae Infection in 9 Rhesus Macaques (Macaca mulatta). *Comp Med*. 2020 1;70:183–189.
6. Ku Y-H, Chuang Y-C, Chen C-C, et al. Klebsiella pneumoniae Isolates from Meningitis: Epidemiology, Virulence and Antibiotic Resistance. *Sci Rep*. 2017 26;7:6634.
7. Kumar V, Sun P, Vamathevan J, et al. Comparative Genomics of Klebsiella pneumoniae Strains with Different Antibiotic Resistance Profiles. *Antimicrob Agents Chemother*. 2011 55:4267–4276.
8. Paczosa MK, Mecsas J. Klebsiella pneumoniae: Going on the Offense with a Strong Defense. *Microbiol Mol Biol Rev*. 2016 80:629–661.
9. Seguel M, Gottdenker NL, Colegrove K, Johnson S, Struve C, Howerth EW. Hypervirulent Klebsiella pneumoniae in California Sea Lions (Zalophus californianus): Pathologic Findings in Natural Infections. *Vet Pathol*. 2017 11;54:846–850.
10. Twenhafel NA, Whitehouse CA, Stevens EL, et al. Multisystemic Abscesses in African Green Monkeys (Chlorocebus aethiops) with Invasive Klebsiella pneumoniae —Identification of the Hypermucoviscosity Phenotype. *Vet Pathol*. 2008 45:226–231.
11. Yang F, Deng B, Liao W, Wang P, Chen P, Wei J. High rate of multiresistant

Klebsiella pneumoniae from human and animal origin. *Infect Drug Resist*. 2019 12:2729–2737.

CASE IV:

Signalment:
4-month-old, female intact (*Mustela putorius furo*) ferret.

History:
A mass was noted in the caudal abdomen and the ferret was euthanized. Coronavirus was suspected.

Gross Pathology:
The adrenal gland is markedly enlarged (up to 3x). The normal parenchyma is extensively replaced by multiple cysts filled with serous fluid, regions of haired skin, and bone /cartilage, which markedly compress a thin rim of adrenal cortex.

Laboratory Results:
No laboratory findings reported.

Microscopic Description:
The adrenal gland is extensively effaced and replaced by a well demarcated, expansile, encapsulated population of neoplastic cells derived from the ectoderm, mesoderm, and (suspected) endoderm. Ectodermal components occupy 60% of the mass and consist of attenuated stratified squamous epithelium that lines a large cystic space filled with lamellated keratin, eosinophilic fluid, degenerate neutrophils, and foamy macrophages. The underlying dermis contains dilated hair follicles, sebaceous glands, and dilated apocrine glands overlying sheets of well-differentiated adipose tissue. A second type of cyst occupying 10% of the mass is lined by an attenuated simple columnar to cuboidal ciliated epithelium with rare goblet cells and is filled with eosinophilic and basophilic flocculent material, foamy macrophages, and karyorrhectic debris. This mass markedly compresses a thin rim of remnant adrenocortical cells characterized by sheets of eosinophilic foamy polygonal cells with central round nuclei. Mesodermal components occupy 30% of the mass and consist of large islands of mature trabecular bone lined by a single layer of osteoblasts surrounded by bone marrow, rare partially mineralized islands of cartilage, and dense fibrous connective tissue.

Contributor's Morphologic Diagnoses:
Adrenal: teratoma, ferret (*Mustela putorius furo*)

Contributor's Comment:
Teratomas are germ cell neoplasms derived from at least two of the three embryonic germ layers: the ectoderm (that gives rise to epithelia, adnexa, and the nervous system), the mesoderm (connective tissue, musculoskeletal, urogenital, and cardiovascular system) and the endoderm (gastrointestinal epithelium, respiratory glandular epithelium, liver, and pancreas).[1] In domestic animals, the majority of teratomas occur in the gonads

Figure 4-1. Adrenal gland, ferret. The adrenal gland is enlarged. Upon section, large cysts containing hair shafts and a focal area of bone (left) are visible. (*Photo courtesy of* : Michigan State University VDL, 4125 Beaumont Road, Lansing, MI 48910-8104.)

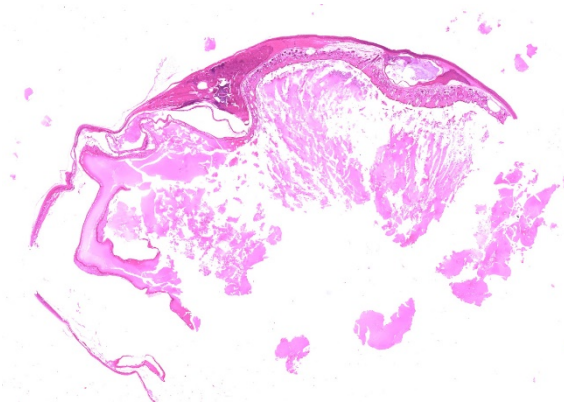

Figure 4-2. Adrenal gland, ferret. Subgross magnification of the submitted gland demonstrates a large central cyst containing abundant proteinaceous granular fluid and debris, bordered dorsally by well-differentiated haired skin and a focal area of bone. (HE, 5X)

but interestingly in ferrets, teratomas most commonly arise within the adrenal gland.[5] In one report of adrenal teratomas in four ferrets, the majority of neoplasms contained tissues form all three germ cell layers including bone, bone marrow, cartilage, teeth, haired skin, brain tissue, peripheral nerves, respiratory epithelium, and gut epithelium. They reported that teratomas were rarely bilateral and rarely metastasized to the mesenteric lymph node.[14] The histogenesis of extra-gonadal teratomas is unclear; however, neoplastic cells are thought to arise from diploid pluripotent precursor cells.[13] In addition to ferrets, adrenal teratomas have been reported in humans, an ox, and a rat.[6,7,11]

In the ferret, gross differentials for an adrenal mass include (from most to least common): adrenocortical hyperplasia, carcinoma, adenoma, pheochromocytoma, leiomyoma/sarcoma, spindle cell sarcoma, and neuroblastoma.[2] Adrenal teratomas are not hormonally active. They are therefore, easy to clinically differentiate from adrenocortical tumors and/or hyperplasia, which produce excess estrogen and estrogen precursors. The excess estrogen induces the telltale signs of adrenal-associated endocrinopathy including bilaterally symmetric truncal alopecia, pruritis, vulvar swelling, inappropriate sexual behavior (neutered males), and dysuria

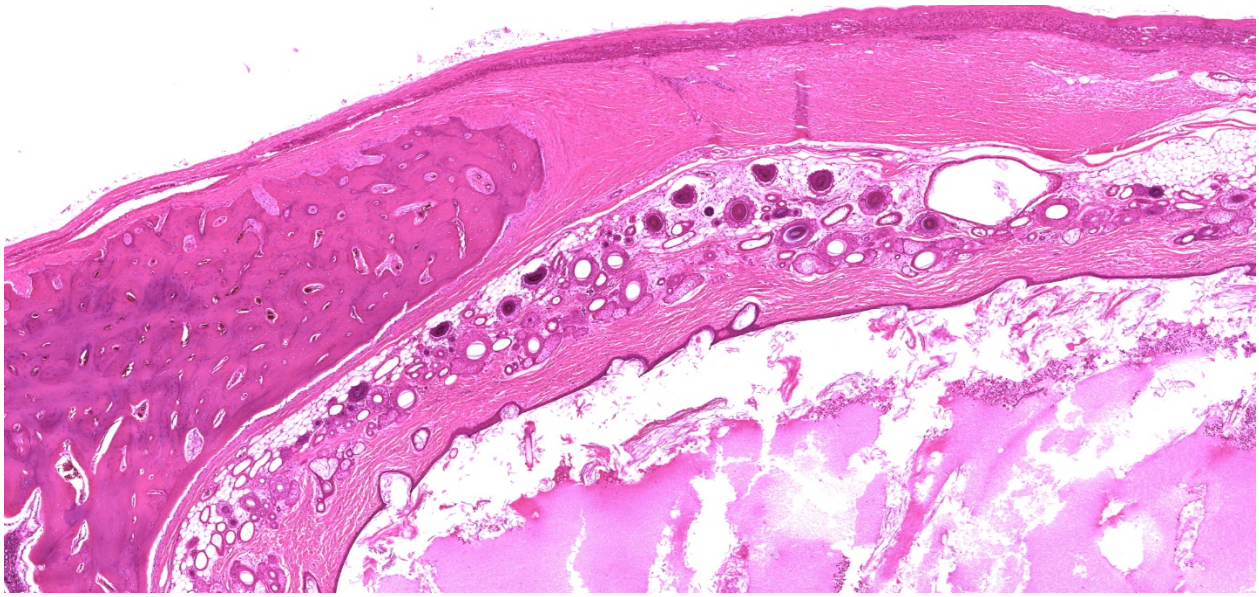

Figure 4-3. Adrenal gland, ferret. Higher magnification demonstrating (from top to bottom): adrenal capsule and thin rim of adrenocortical cells, mesodermal fibrous connective tissue containing well-formed bone and marrow (bottom left), a thick segment of well differentiated haired skin, and a cystic area containing abundant granular proteinaceous debris, lamellar keratin debris, and aggregates of neutrophils. (HE, 33X)

(males).[9] Histologically, while differentiating between adrenocortical hyperplasia vs carcinoma vs adenoma is challenging, distinguishing these entities from teratomas is straightforward.

In this case, while there is clear differentiation into ectodermal and mesodermal components, suspected endodermal components are limited to the dilated cyst lined by ciliated columnar to cuboidal epithelium with goblet cells, which may represent some form of respiratory epithelium. Given that only two germ cell layers are confirmed in this case, a differential diagnosis to consider is a dermoid cyst. Dermoid cysts are defined as mature teratomas composed predominantly of a cyst lined by stratified squamous epithelium variably filled with lamellated keratin and associated with hair follicles, sebaceous glands, and apocrine glands. Less prominent components of the mass may include bone, cartilage, fat, or muscle.[8] Teratoma remained the favored diagnosis in this case given that adrenal teratomas are a well-established entity in ferrets; adrenal dermoid cysts are rarely reported in the literature and have not been described in the ferret.

Contributing Institution:
Michigan State University
https://cvm.msu.edu/vdl

JPC Diagnosis:
Adrenal gland: Teratoma.

JPC Comment:
This case represents a classic presentation of this entity in ferrets, while the gonads are the most commonly affected location in other domestic species.

Reports of neoplasms likely to be teratomas (or dermoid cysts) have been found in ancient literature, with the earliest likely description of a teratoma being found on a Babylonian cuneiform papyrus dating to 2,000 B.C. Galen also described a lesion likely a dermoid cyst during the first century A.D. The first unequivocal description of an ovarian dermoid cyst was published by Johannes Scultetus in 1659, describing the results of an autopsy of a woman with an ovarian tumor. However, Leblanc first used the term "dermoid cyst" while describing a lesion in the base of a horse's skull, emphasizing its gross resemblance to skin. The first to describe the microscopic features of dermoid cysts was Kohlrausch in 1843, who noted their histologic resemblance to skin. The term "teratoma" (*teras*; Greek for "monster") was first introduced by Rudolf Virchow in 1863, in the first edition on his book on tumors. As noted by the contributor, both terms are still in use today, with dermoid cysts restricted to dermal and epidermal elements (both composed of ectoderm) while teratomas also comprise mesodermal and endodermal elements.[10]

During the Middle Ages, teratomas were thought to arise due to sins of the flesh, which is unsurprising given their often striking gross features. This notion was further supported in that the lesion often resembled a deformed fetus, strengthening suspicion that teratomas were the result of wicked sins such as fornication with the devil, sexual fantasies and dreams, and witchcraft. One account

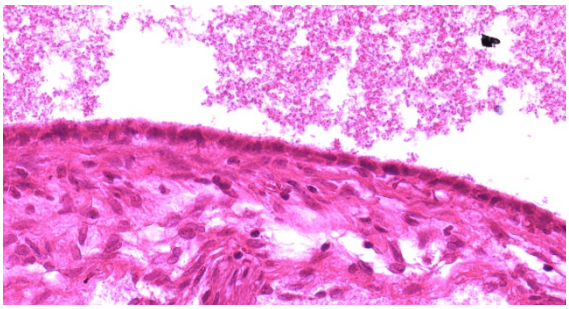

Figure 4-4. Adrenal gland, ferret. One smaller cyst is lined by attenuated ciliated respiratory epithelium (HE, 617X)

describes "…a male child developed so completely in the thigh of its father, …as to permit being brought into the world alive by an operation at the end of nine months." The report went on to discuss the need for baptism in such cases. Multiple theories have subsequently arisen over the following centuries to their cause, including a prerequisite of sexual relations, consumption of human teeth and bones, in situ pregnancies induced by misery and disgrace, a parasitic fetus, and parthenogenesis.[10]

In companion animals, teratomas are most commonly benign but can also be malignant with distant metastasis of one or more of the components. The histogenesis of these neoplasms likely varies depending on the site of origin. Gonadal teratomas thought to develop from parthenogenetic development of haploid post-meiotic germ cells or diploid premeiotic germ cells whereas extragonadal teratomas likely originate from undifferentiated diploid pluripotent progenitor cells. Although the incidence of extragonadal teratomas is very low, they are not restricted

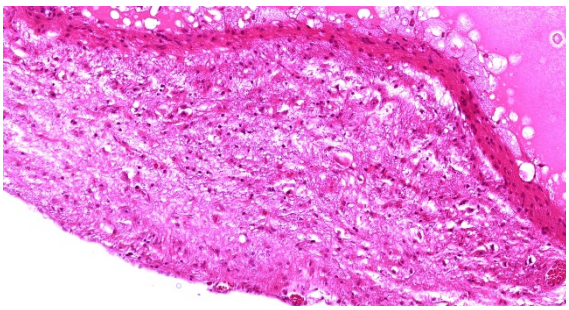

Figure 4-5. Adrenal gland, ferret. A strip of nervous tissue is also present in the neoplasm. (HE, 176X)

to the adrenal gland. Non-adrenal extragonadal teratomas are typically congenital, found along the midline, and have been reported in humans, ducks, rabbits, rats, mice, an ox, a kitten, a sheep, a calf, and a blue heron.[14]

Interestingly, the first case of malignant testicular teratoma (i.e. testicular teratocarcinoma) in a ferret was recently reported in a 7 month old ferret that initially presented for an enlarged left testicle. The testicular mass was later found to be a teratoma with all three germ cell lines. The ferret subsequently developed an abdominal mass initially suspected to be an adrenocortical tumor and

Table 1[4,12]

Ectoderm	Mesoderm	Endoderm
• Epidermis of skin and its derivatives (sweat glands, hair follicles, and sensory receptors) • Epithelial lining of mouth and anus • Cornea and lens of eye • Nervous system • Adrenal medulla • Tooth enamel • Epithelium of pineal and pituitary glands	• Notochord • Musculoskeletal system • Muscular layer of stomach and intestine • Excretory system • Circulatory and lymphatic systems • Reproductive system (except germ cells) • Dermis of skin • Adrenal cortex	• Epithelial linings (digestive tract, respiratory system, urethra, urinary bladder, and reproductive system) • Liver • Pancreas • Thymus • Thyroid and parathyroid glands

was euthanized following a decline in health over the following weeks. Upon histologic examination of the tissues, metastasis of the poorly differentiated epithelial component were identified in multiple tissues, including the urinary bladder, ureters, prostate, pelvic fat, abdominal and thoracic lymph nodes, kidney, and lung.[3]

Participants discussed the multitude of tissues derived from the embryonic germ cell layers, which were previously outlined in 2013 WSC#8, case 3 and are reflected in Table 1.

References:

1. Agnew DW, MacLachlan NJ. Tumors of the genital systems. In: Meuten DJ, ed. *Tumors in Domestic Animals.* 5th Ames, IA: John Wiley & Sons, Inc.; 2017:690-698.
2. Avallone G, Forlani A, Tecilla M, et al. Neoplastic diseases in the domestic ferret (Mustela putorius furo) in Italy: classification and tissue distribution of 856 cases (2000-2010). *BMC Vet Res* 2016, 12(1):275.
3. Fiddes KR, Murray J, Williams BH. Testicular Teratocarcinoma in a Ferret (Mustela putorius furo). *J Comp Pathol*. 2020;181:63-67.
4. Foster RA. Male reproductive system. In: McGavin MD, Zachary JF, eds. *Pathologic Basis of Veterinary Disease*. 6th ed. St. Louis, MO: Elsevier; 2017:1210-1211.
5. Fox JG, Muthupalani S, Kiupel M, Williams B. Neoplastic diseases. In: Fox JG, Marini RP, eds. *Biology and Diseases of the Ferret*. 3rd ed. New York, NY: John Wiley & Sons Inc.; 2014:595.
6. Ladds PW, Russell P, Foster RA: Adrenal teratoma in an ox. *Aust Vet J* 67:464–465, 1990.
7. Lam KY, Lo CY. Teratoma in the region of the adrenal gland: a unique entity masquerading as lipomatous adrenal tumor. *Surgery* 126:90–94, 1999.
8. Mensi DW. Cytologic findings in two cases of dermoid cysts with malignant transformation. *Diagnostic Cytopathology* 2011, 39(12):919-923.
9. Miller CL, Marini RP, Fox JG. Diseases of the Endocrine System. In: Fox JG, Marini RP, eds. *Biology and Diseases of the Ferret*. 3rd ed. New York, NY: John Wiley; 2014:377-380.
10. Pantoja E, Noy MA, Axtmayer RW, Colon FE, Pelegrina I. Ovarian dermoids and their complications. Comprehensive historical review. Obstet Gynecol Surv. 1975 Jan;30(1):1-20.
11. Schardein JL, Fitzgerald GE. Teratoma in a Wistar rat. *Lab Anim Sci* 27:114, 1977
12. Schlafer DH, Foster RA. Female genital system. In: Maxie MG, ed. *Jubb Kennedy and Palmer's Pathology of Domestic Animals*. Vol 3. 6th ed. Philadelphia, PA: Elsevier Saunders; 2016:377-378.
13. Wagner H, Baretton GB, Scheiderbanger K, Nerlich A, Bise K, Lohrs U. Sex chromosome determination in extragonadal teratomas by interphase cytogenetics: clues to histogenesis. *Pediatr Pathol Lab Med* 17:401–412, 1997.
14. Williams BH, Yantis LD, Craig SL et al. Adrenal teratoma in four domestic ferrets (Mustela putorio furo). Path. 2001, 38:328-331.